ANTIOXIDANTS & REDOX SIGNALING
Volume 11, Number 9, 2009

DOI: 10.1089/ars.2008.2355

New Treatment of Periodontal Diseases by Using NF-κB Decoy Oligodeoxynucleotides *via* Prevention of Bone Resorption and Promotion of Wound Healing

Hideo Shimizu,[1,2] Hironori Nakagami,[3] Shosuke Morita,[4] Ikuyo Tsukamoto,[5] Mariana Kiomy Osako,[1,2] Futoshi Nakagami,[1,2] Takashi Shimosato,[6] Noriko Minobe,[6] and Ryuichi Morishita[2]

Abstract

Nuclear factor-kappa B (NF-κB) is involved in osteoclast differentiation and activation. Thus, the blockade of the NF-κB pathway might be a novel therapeutic strategy for treating bone metabolic diseases. Periodontitis is subgingival inflammation caused by bacterial infection; this disease also is thought to be a chronic focal point responsible for systemic diseases. In this study, NF-κB decoy oligodeoxynucleotides (ODNs) were topically applied for experimental periodontitis in a debris-accumulation model and wound healing in a bone-defect model of beagle dogs to investigate the effect of decoy ODN on bone metabolism. Application of NF-κB decoy ODN significantly reduced interleukin-6 activity in crevicular fluid and improved alveolar bone loss in the analysis of dental radiographs and DEXA. Direct measurement of exposed root that lost alveolar bone support revealed that NF-κB decoy treatment dramatically protected bone from loss. In a bone-defect model, NF-κB decoy ODN promoted the healing process as compared with control scrambled decoy in micro-CT analysis. Overall, inhibition of NF-κB by decoy strategy prevented the progression of bone loss in periodontitis and promoted the wound healing in bone defects through the inhibition of osteoclastic bone resorption. Targeting of NF-κB might be a potential therapy in various bone metabolic diseases. *Antioxid. Redox Signal.* 11, 2065–2075.

Introduction

Periodontal disease is initiated by an inflammatory response caused by infection of a periodontal pocket arising from the accumulation of subgingival plaque (2, 16, 22). In association with the infection, bacterial antigen and lipopolysaccharides (LPSs) weaken connective-tissue attachments in the gigiva and induce an immune response in the subgingival crevicular fluid. Multiple cytokines such as interleukin (IL)-1, IL-6, and tumor necrosis factor-alpha (TNF-α) are involved in this response. As the inflammation advances, these cytokines in crevicular fluid induce differentiation of osteoclasts from their precursors, leading to bone resorption and destruction adjacent to the root and eventually to tooth loss (2, 14, 25). An edentulous condition causes malfunction of oral mastication and pronunciation, leading to deterioration in daily activities. Periodontal disease also has been considered a possible risk factor for other systemic diseases, such as cardiovascular disease and pre-term low-birth-weight infants, as well as the development of diabetes mellitus (7, 17, 18, 27). Several approaches (brushing, scaling, and antibacterial paste) have been used to prevent the initiation and the progression of inflammation, and surgical operation is often performed in severe cases with advanced inflammation (3).

The transcription factor NF-κB plays a pivotal role in the coordinated transactivation of cytokine and adhesion-molecule genes involved in such conditions. Recently, inhibition of NF-κB by decoy ODN was proven to be effective against osteoclast differentiation and activation in an *in vitro* study (20), and peritoneal administration of NF-κB decoy ODN *in vivo* attenuated bone resorption and destruction of the femur and tibia in ovariectomized rats, an osteoporosis model (20). As inhibition of NF-κB by local administration of decoy ODN was also effective to treat rheumatoid arthritis (26), it is noteworthy to use the decoy approach for the treatment of bone loss due to inflammation and for the promotion of wound healing in bone defects. In this study, topical administration of NF-κB decoy ODN was used as a novel

Departments of [1]Geriatric Medicine, [2]Clinical Gene Therapy, and [3]Gene Therapy Science, Osaka University Graduate School of Medicine, Suita; and [4]First Department of Oral and Maxillofacial Surgery, Osaka Dental University, Hirakata, Osaka; [5]Department of Food Science and Nutrition, Nara Women's University, Nara; and [6]Research Department, NISSEI BILIS Co. Ltd., Koga, Shiga, Japan.

therapy to prevent the inflammatory process in periodontal disease and to prevent bone destruction with tooth loss and focal infection and subsequent systemic diseases.

Material and Methods

Animals

These experiments were approved by the Animal Ethics Committee at NISSEI BILIS, Shiga, Japan, and carried out on 1-year-old beagle dogs. Twelve male beagle dogs were divided in three groups for analysis at 1, 2, and 3 months (four dogs per group). All surgical procedures were performed under general anesthesia with sodium pentobarbital (Nembutal; Dainippon Sumitomo Pharma, Osaka, Japan) and local injection of 2% xylocaine.

NF-κB decoy ODNs

NF-κB or scrambled ODNs were as follows:

NF-κB decoy ODN: (consensus sequences are underlined), as previous described (26).
5′-CCTTGAAGGGATTTCCCTCC-3′
3′-GGAACTTCCCTAAAGGGAGG-5′
Scrambled decoy ODN:
5′-TTGCCGTACCTGACTTAGCC-3′
3′-AACGGCATGGACTGAATCGG-3′

Synthetic ODNs were washed with 70% ethanol, dried, and dissolved in sterile Tris-EDTA (10 μM Tris, 1 μM EDTA), and the supernatant was purified over a NAP 10 column (Pharmacia, Piscataway, NJ).

Periodontitis in debris-accumulation model

All second incisors were ligated in the cervical area in the gingival sulcus with surgical 2.0 silk thread to induce debris accumulation in a modified model of periodontitis (10, 11). NF-κB decoy ODNs (1 mg) were injected into subgingival area of alveolar bone proximal to the second incisors in the left upper and lower jaw every 2 weeks for 1, 2, or 3 months. As control, scrambled decoy ODNs were injected into the right-side second-incisor subgingival area in the same amount. Dental radiographic examination was performed every 2 weeks to evaluate bone loss in the alveolar region. At 1, 2, and 3 months, the frontal areas of the upper and lower jaws were excised *en bloc* for further analysis with DEXA and the measurement of root exposure.

IL-6 in gingival fluid

At 1 month, the surgical threads at the cervix were removed, and subgingival fluid in the sulcus around the second incisors was collected with a microtube. IL-6 in the fluid was measured with EIA (Quantikine Immunoassay; R&D Systems, Minneapolis, MN).

Alveolar-to-root length

As the alveolar length taken in x-ray film varies depending on the angle between the film plane and the x-ray source, being sometimes elongated and sometimes shortened, we used the ratio of the alveolar length to the root length as a control that was stable during the experimental period. Then the ratio of alveolar bone length to root length was calculated to evaluate the remaining alveolar bone height.

Root-exposure length

In some samples, organic tissue was removed with sodium hypochlorite to expose the root and alveolar bone. The length of the root between the cervix and the ridge of the alveolar process that had lost bone support was measured as the root-exposure length. In this sample, direct measurement was performed on both the buccal and lingual sides of the second incisors in the upper and lower jaws.

Wound healing in the bone-defect model

Wound healing in a surgically created bone-defect model was based on the modification of previous reports (13,19). Besides general anesthesia with Nembutal, local injection of 2% xylocaine was performed under the gingiva in the area of the first molars. A surgical incision was made at the alveolar ridge along the cervical level of the first premolar to the second molar, and a horizontal incision also was made in both ends, and the gingiva was peeled off as a mucoperiosteal flap to expose the alveolar bone surface and clear the operation area. An artificial bone defect 3 mm in diameter was surgically created with a dental steel bur under the bifurcation in the buccal area of the first molar. After compression hemostasis of the surgical defect, the NF-κB decoy ODN (4 mg) was applied on the left side, and a scrambled decoy ODN on the right side, in the same manner. The wound was closed by suturing the flap over the created bone defect, and the sutures were removed 1 week after the operation. At 1, 2, and 3 months, the dogs were killed under deep anesthesia with an overdose of pentobarbital (Nembutal). The upper and lower jaws from the mesial side of the first premolar to the distal side of the second molar were excised with a surgical saw in one block and fixed with 70% ethanol for further analysis.

Dual-energy x-ray absorptiometry

Bone-density measurements were performed by using dual-photon x-ray absorbsiometry (DEXA) bone densitometry (GE-Lunar DPX-IQ; Madison, WI). The targeted area was selected in the alveolar bone process between the incisors and the adjacent tooth. High- and low-beam energies for all scans were 80 kV and 35 kV, respectively, at 0.5 mA, as previously described (28). Bone-mineral density (BMD) was obtained in grams per square centimeter.

Micro-computed tomography

The bone microarchitecture was analyzed by using cone-beam micro-computed tomography (x-ray CT system, SMX-100CT-SV; Shimazu, Kyoto, Japan) and software (TRI/3D-BON; RATOC System Engineering Co., Ltd., Tokyo, Japan), which serves as a valuable tool for evaluating the structure in the trabecular bone. In brief, alveolar bone was scanned at the bone-defect region under the bifurcation of the first molar. A total of 135 consecutive tomographic slices was obtained with a slice thickness of 12.8 μm at 8-μm resolution. After scanning, three-dimensional microstructual image data were reconstructed, and structural indices were calculated by using 3D trabecular bone-analysis software, TRI/3D-BON, as previously described (23). Gray-scale images were segmented

by using a median filter to remove noise and by using a fixed threshold to extract the mineralized bone phase. Subsequently, the isolated small particles in the marrow space and the isolated small holes in the bone were removed by using a cluster-labeling algorithm. The trabecular bone was then separated, and structural indices were analyzed. Bone volume (BV) was calculated by using tetrahedrons corresponding to the enclosed volume of the triangulated surface. Total tissue volume (TV) was the volume of the entire scanned sample. Trabecular bone-volume fraction was calculated from these values.

Cell cultures

Human osteoblasts were obtained from Cell Applications (San Diego, CA). Bone marrow–derived mononuclear cells, which contain both osteoblasts and osteoclast precursors, were obtained from 3-day-old neonatal white rabbits, as previously described (20). In brief, rabbit bone marrow cells were flushed from the femurs and tibias, collected into tubes, and washed twice with PBS. The mononuclear cell–rich fraction was separated from marrow cells by density-gradient centrifugation with Ficoll and cultured (1×10^5 cells per well of a 24-well plate) in α-MEM medium containing 10% fetal bovine serum. These cells were stimulated with LPS (1 μg/ml; Sigma) or vitamin D_3 (1×10^{-7} *M*; Sigma) or Osteogenic medium containing dexamethasone and ascorbate and β-glycerophosphate (Lonza, Walkersville, MD) and further treated with NF-κB decoy ODN or scrambled decoy ODN (0.5 μ*M*) for the following assessments. For transfection of ODN, we put NF-κB decoy ODN or scrambled decoy ODN (0.5 μ*M*) into culture medium in bone marrow–derived mononuclear cells, as previously described (20), and used LipofectAMINE2000 (Invitrogen, Grand Island, NY) in human osteoblast cells.

Real-time reverse transcription–polymerase chain reaction

Human osteoblasts stimulated with LPS or Osteogenic medium in addition to NF-κB or scrambled decoy ODN for 24 h were assessed for alkaline phosphatase (ALP), osteocalcin, monocyte chemotactic protein (MCP)-1, IL-6, and RANKL expression with the real-time reverse transcription–polymerase chain reaction (RT-PCR). Total RNA of cells or tissue samples was extracted by using RNeasy Mini Kit (Qiagen) or the Isogen (Nippon Gene, Toyama, Japan). Complementary DNA was synthesized by using the Thermo Script RT-PCR System (Invitrogen, Carlsbad, CA). Relative gene-copy numbers of RANKL, OPG, and glyceraldehyde-3-phosphate dehydrogenase (GAPDH) were quantified with real-time RT-PCR by using TaqMan Gene Expression Assays (human RANKL, Hs00243522; osteocalcin, Hs00609452; alkaline phosphatase, Hs00758162; Eukaryotic 18S rRNA (18S), 4352930E; Applied Biosystems, Foster City, CA). The absolute number of gene copies was normalized by using GAPDH and standardized by a sample standard curve.

Tartrate-resistant acid phosphatase and alizarin red staining

After treatment with Osteogenic medium and vitamin D_3 for 2 weeks, rabbit bone marrow culture medium were measured for ALP and TRAP activity, and the ALP-to-TRAP ratio was calculated as a evaluation of the total balance of osteoblast and osteoclast activity in the process of calcification, as previously described (21). Bone marrow cells were fixed with 4.0% paraformaldehyde in PBS for 10 min at room temperature before being stained for TRAP as osteoclast identification. Enzyme histochemical staining for TRAP and Hoechst 33526 nuclear staining were performed, as previously reported (20). In some cultures, bone marrow was continuously maintained with Osteogenic medium and vitamin D_3, and in 4 weeks, *in vitro* calcification was detected with alizarin red staining, according to the Dahl's method.

Statistical analysis

All values are expressed as mean + SEM. Analysis of variance with subsequent Bonferroni/Dunnett tests was used to determine the significance of differences in multiple comparisons. Values of $p < 0.05$ were considered to be statistically significant.

Results

Periodontitis in debris-accumulation model

In this model, periodontitis was initiated with bacterial infection due to debris accumulation caused by a thread tied around the cervix. Accordingly, several cytokines were induced in the subgingival sulcus, which led to destruction of the gingival attachment and to alveolar bone resorpiton around the tooth, as shown in Fig. 1A. Direct measurement of the incisor roots, where bone support was lost, was performed on both the buccal and lingual sides. Root-exposure length increased in a time-dependent manner, indicating an advance of bone destruction by inflammation induced by debris accumulation (Fig. 1A–C).

To investigate the mechanism of alveolar bone resorption in the debris-accumulation model, we initially focused on IL-6 in the subgingival sulcus fluid as a major cytokine that induces osteoclasts to engage in bone resorption (15). Direct administration of NF-κB decoy ODN (1 mg/0.2 ml saline), around the root region of second incisors (Fig. 1B), decreased the concentration of IL-6 in the subgingival sulcus fluid compared with that of the scrambled decoy ODN–administrated side in both the upper and lower jaws ($p < 0.01$), as shown in Fig. 2.

Dental radiographs were taken in every 2 weeks, and the remaining alveolar bone was evaluated as the ratio to the root length, which was stable during the experiment (Fig. 3A). Alveolar bone supporting incisors was resorbed in a time-dependent manner by the inflammation induced by debris accumulated because of surgical threads tied in the cervix of the second incisors (Fig. 3B). In the group with scrambled decoy ODN injection, alveolar bone was reduced to ~83% of the original height at 1 month and gradually advanced to 66% at 3 months in the upper jaw. In the lower jaws, in the group with scrambled decoy ODN, bone loss was clearly decreased to 49% of the original length at 3 months. In contrast, in the group with NF-κB decoy ODN injection, alveolar bone in the area of incisors was well preserved: ~91% of the original height at 2 months and >80% even at 3 months in the upper jaw and >60% at 3 months in the lower jaw (Fig. 3C). These results demonstrate that NF-κB decoy ODN protected against bone loss as compared with scrambled decoy ODN.

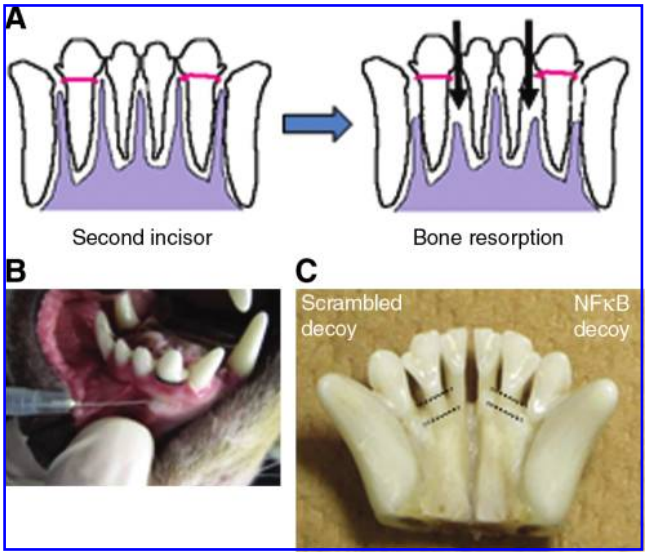

FIG. 1. Induction of periodontis in debris-accumulation model with ligation of second incisors. (**A**) **Upper panel**, Scheme of alveolar bone resorption induced by inflammation with debris accumulation and bacterial infection. (**B**) The picture demonstrates injection of NF-κB or scrambled decoy ODN (1 mg/0.2 ml) into the subperiosteal bone region in the root area of the second incisors. NF-κB decoy ODN was injected in the left upper and lower jaws, and scrambled decoy ODN, in the right upper and lower jaws. (**C**) A representative picture of the frontal portion of the lower jaws at 2 months in the debris-accumulation model. Gingiva and mucoperiosteal organic tissue were removed with sodium hypochlorite.

In the direct measurement of the incisor roots on both the buccal and lingual sides, root-exposure length was markedly observed in the group with scrambled decoy ODN administration, and bone loss had increased to 3.0 mm in the upper jaw and 4.2 mm in the lower jaw on the lingual side at 3 months. In contrast, alveolar bone support was well preserved in the side with the NF-κB decoy ODN administration; bone loss was reduced to as little as 2.2 mm in the upper jaw and 3.1 mm in the lower jaw in the same site, indicating that alveolar bone resorption was attenuated by NF-κB decoy ODN (Fig. 3D).

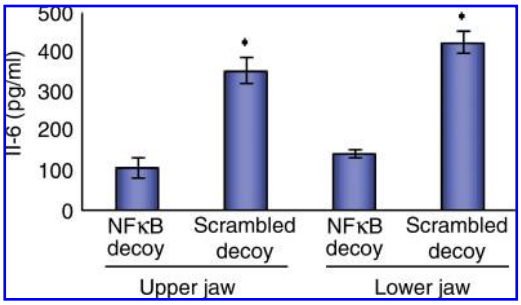

FIG. 2. IL-6 (picograms per milliliter) in the subgigival sulcus fluid of second incisors 1 month after ligation of second incisors in upper and lower jaws. NF-κB decoy ODNs were injected in the left-side jaws, and scrambled decoy ODNs in the right-side jaws. $*p < 0.01$ *versus* NF-κB decoy ODNs.

DEXA analysis was performed in the area of alveolar bone that supports the roots of the incisor and adjacent tooth (Fig. 4A). Because dental radiographic examination in this experiment was two-dimensional analysis, measuring the bone density with DEXA was also a useful approach to confirm the data. Bone-mineral density gradually decreased with time and was reduced to 0.21 g/cm^2 at 1 month and to 0.13 g/cm^2 at 3 months in the upper jaw in the scrambled decoy ODN–treated site. In contrast, bone-mineral density was significantly well preserved −0.29 g/cm^2 at 1 month and 0.18 g/cm^2 at 3 months in the NF-κB decoy ODN–treated site ($p < 0.01$) (Fig. 4B). These results support that NF-κB decoy ODN treatment protects bone mineral from resorption due to inflammation induced by debris as compared with scrambled decoy ODN treatment.

Wound healing in the bone-defect model

To evaluate the effect of NF-κB decoy ODN on bone metabolism, we used another model of wound healing surgically created in alveolar bone (Fig. 5). In this model, an alveolar bone defect was closed over with a mucoperiosteal flap of gingiva, and the defect gradually filled with newly formed bone after the initial inflammation.

In dental radiographic films shown in Fig. 6, the healing process was visually confirmed by calcification in the defect area created under the bifurcation of the first molars, where the defect area was covered earlier in the topical NF-κB decoy ODN–treated side. At 1 month after treatment, in the sample of mucoperiosteal gingival tissue removed, cortical hard bone already covered the defect area in the topical NF-κB decoy ODN–treated side, whereas weak, fragile soft bone was observed in the scrambled decoy ODN–treated site, which indicated early calcification with NF-κB decoy–ODN treatment (Fig. 7).

DEXA analysis was performed in the area of alveolar bone under the bifurcation of the first molars in which calcification occurred during the process of wound healing (Fig. 8A). As was seen in the series of dental radiographic examinations (Fig. 6), bone-mineral density gradually increased with time and recovered to 0.31 g/cm^2 at 1 month and to 0.42 g/cm^2 at 3 months in the lower jaw in the scrambled decoy ODN–treated site. In contrast, bone-mineral density was markedly and significantly increased to 0.41 g/cm^2, even at 1 month, and recovered to 0.46 g/cm^2 at 3 months in the NF-κB decoy ODN–treated site ($p < 0.05$; Fig. 8B). These results suggest that NF-κB decoy–ODN treatment promoted calcification in the wound healing of a surgically created bone defect, in comparison with scrambled decoy ODN treatment.

We also used micro-CT, which allowed analysis of trabecular formation in relation to bone metabolism in the selected area of created bone defect. At 1 month after surgery, a three-dimensional reconstruction image of trabecular bone in the defect area demonstrated that very little bone formation was observed in the scrambled decoy ODN–treated site in both the horizontal and vertical views, whereas thick trabecular bones occupied the defect area in the NF-κB decoy ODN–treated site (Fig. 9A). In micro-CT analysis, the bone-volume to total-volume ratio (BV/TV), which indicates the percentage recovery of trabecular bone structure in the total space in

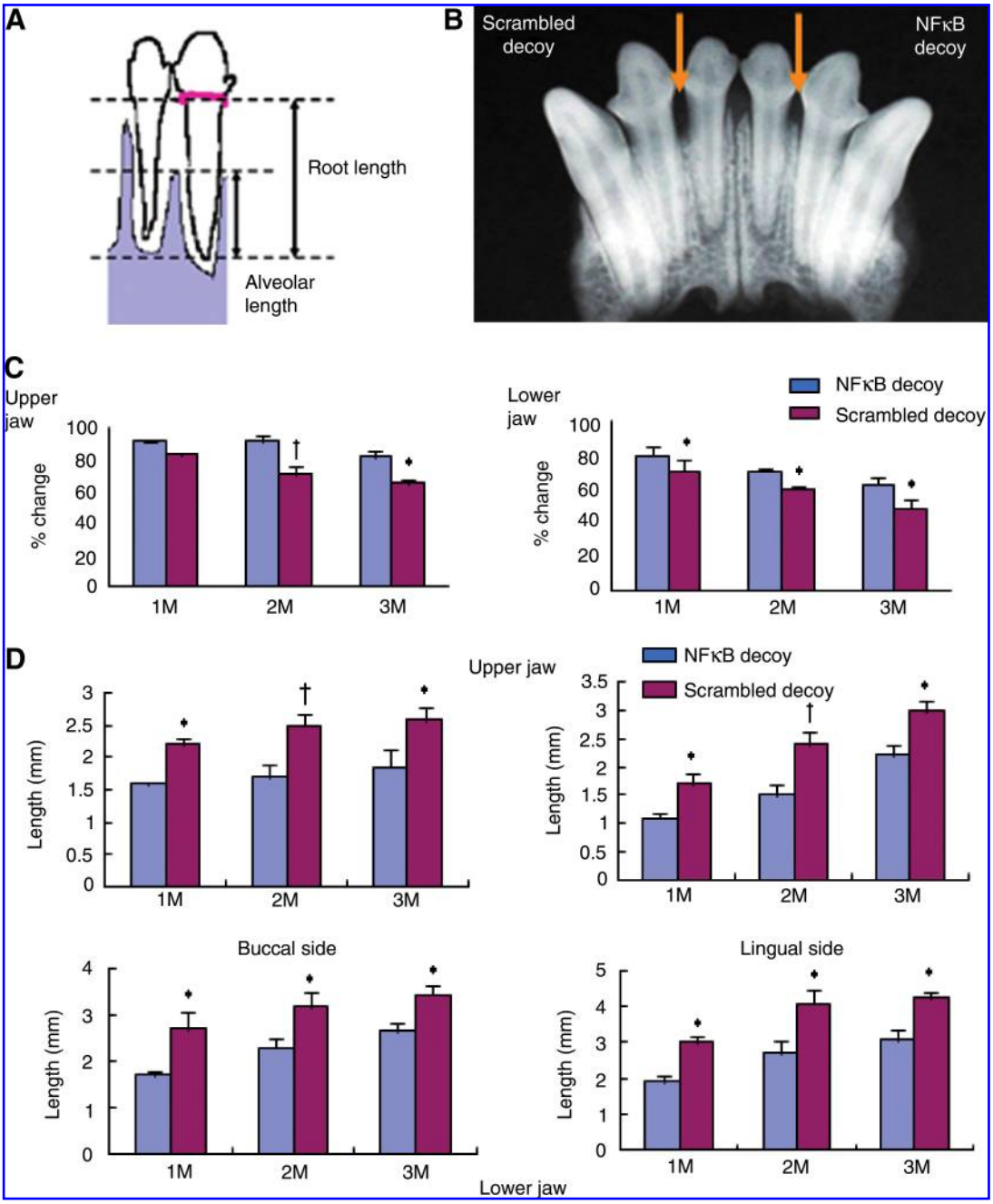

FIG. 3. Alveolar bone evaluation at 1, 2, and 3 months (1, 2, and 3M) after ligation of second incisors. (**A**) The scheme shows the measurement points to evaluate the remaining alveolar bone. (**B**) A representative dental radiographic film of the lower frontal jaw at 1 month in the debris-accumulation model. (**C**) The percentage change in ratio of alveolar bone height to root length (percentage) in upper and lower jaws. *$p < 0.05$ *versus* NF-κB decoy ODNs. †$p < 0.01$ *versus* NF-κB decoy ODNs. (**D**) Length of exposed root with loss of alveolar bone support at 1, 2, and 3 months (1, 2, and 3M) after ligation of second incisors. The length of exposure roots (in millimeters) of the second incisors on the buccal and lingual sides in the upper and lower jaws. *$p < 0.05$ *versus* NF-κB decoy ODNs.

volume, was used to evaluate calcification in the healing process. Statistical analysis of bone volume occupying the space demonstrated that 35.6% of the space was occupied at 1 month, gradually increasing to a plateau of 70.7% at 3 months in the scrambled decoy ODN–treated site. In contrast, 48.6% of the space was already occupied by newly formed trabecular bone at 1 month, and 67.4% of the space was filled with bone at only 2 months in the NF-κB decoy ODN–treated site (Fig. 9A). This finding was also confirmed by histologic examination in the mesial–distal section in which new trabecular were observed dispersed in the bone-defect area in the NF-κB decoy ODN–treated site, whereas the defect almost remained intact in the wound area in the scrambled decoy ODN–treated site 1 month after surgical operation (Fig. 9B). This process of recovery was significant in that NF-κB decoy ODN treatment accelerated wound healing, with equal

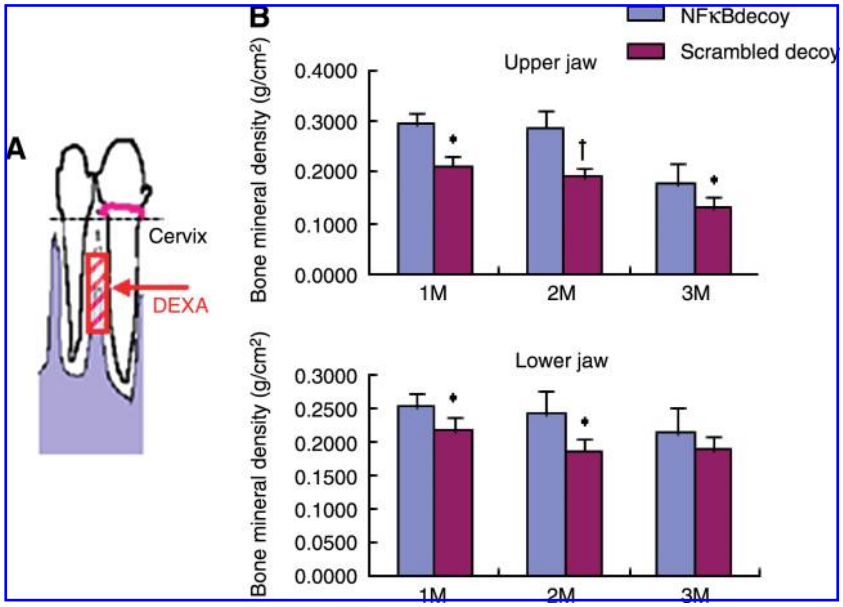

FIG. 4. DEXA analysis of bone-mineral density at 1, 2, and 3 months (1, 2, and 3M) after ligation of second incisors. (**A**) The area of alveolar bone examined with DEXA. (**B**) Bone-mineral density (grams per square centimeter) of upper and lower jaws (**upper** and **lower** panels, respectively). *$p < 0.05$ *versus* NF-κB decoy ODNs; †$p < 0.01$ *versus* NF-κB decoy ODNs.

recovery 1 month earlier than with scrambled decoy ODN treatment. These results confirmed that NF-κB decoy ODN treatment also promoted wound healing in the bone defect in comparison with scrambled decoy ODN treatment.

Molecular mechanism of NF-κB decoy ODN on osteogenesis

To examine the effect of NF-κB decoy ODN on osteogenesis, we used an *in vitro* osteogenic system with human osteoblast cells and bone marrow–derived mononuclear cells with treatment of osteogenic medium. Cell viability, as assessed by MTS assay, was not changed under osteogenic medium treatment in the presence of NF-κB decoy ODN, and scrambled decoy ODN did not affect the viability of the cells (data not shown). In human osteoblast cells, the treatment with osteogenic medium increased the mRNA expression of bone markers, alkaline phosphatase (ALP), and osteocalcin, whereas treatment of NF-κB decoy ODN did not attenuate them (Fig. 10A). LPS stimulation of human osteoblasts enhanced the proinflammatory genes that induced osteoclast formation and activity, such as MCP-1, IL-6, and RANKL, whereas NF-κB decoy ODN significantly attenuated these LPS-induced cytokine expressions (Fig. 10B). These results suggest that NF-κB decoy ODN has no direct effect on osteogenesis in osteoblast cells, although the NF-κB decoy ODN specifically attenuated LPS-induced cytokine expression in human osteoblast cells, which may secondarily affect bone formation by regulating inflammation (12, 29, 30).

In rabbit bone marrow–derived mononuclear cells, continuous treatment with osteogenic medium for 4 weeks induced calcified nodules, assessed with alizarin red staining. Co-treatment with vitamin D_3 inhibited the formation of calcified nodules, whereas co-treatment with vitamin D_3 in the presence of NF-κB decoy ODN induced calcified nodules. Similarly, the ALP-to-TRAP ratio in the culture medium, which reflects the osteogenesis by the balance of osteoblast and osteoclast activity, was increased with the stimulation of osteogenic medium, but not in co-treatment with vitamin D_3. NF-κB decoy ODN attenuated the vitamin D_3–induced reduction in the ratio (Fig. 11). These results suggest that NF-κB decoy ODN may induce osteogenesis by modulating the balance of osteoblast and osteoclast activity. To evaluate the osteoclast activity in this system, we performed TRAP staining, which reflected osteoclast activity. Rabbit bone marrow–derived mononuclear cells with co-stimulation of osteogenic

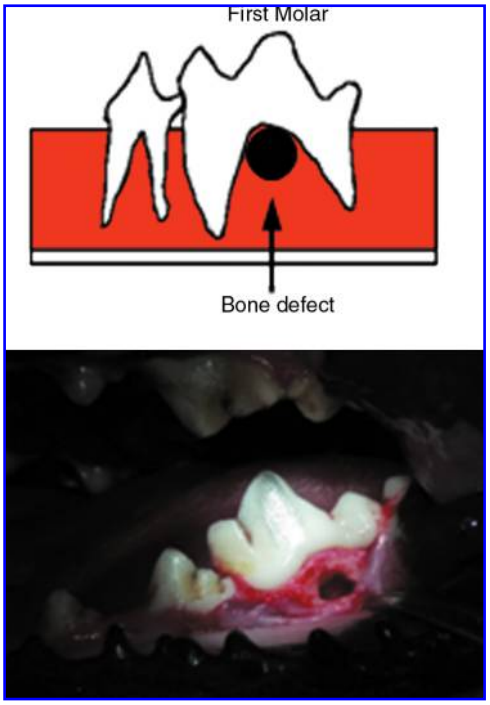

FIG. 5. Creation of bone-defect model. *Upper panel* shows a schematic image of the bone defect (3 mm in diameter) created under the bifurcation of the first molars. *Lower panel* shows a representative picture of surgery to create the bone defect by exposing the alveolar bone surface, with a muco-periosteal flap.

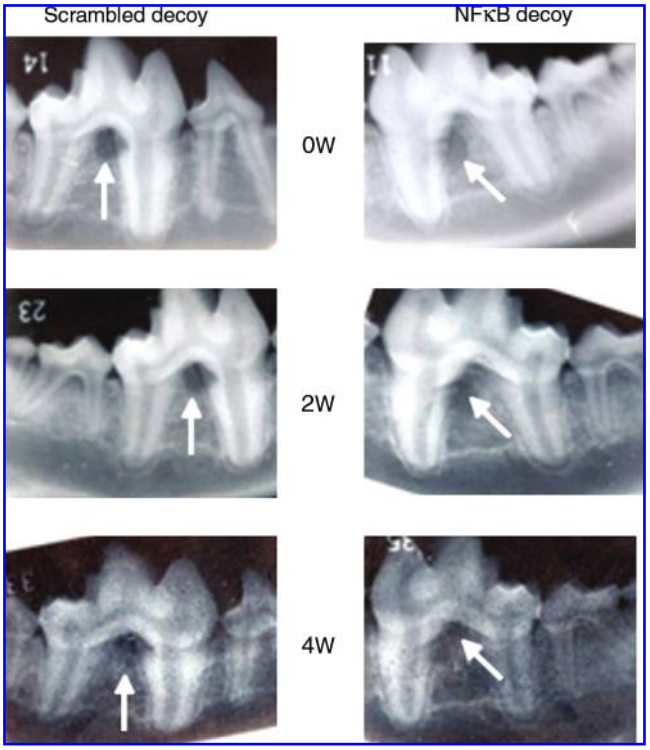

FIG. 6. Representative views of the healing process of the bone-defect region in dental radiographic films at just after, and at 2 and 4 weeks (0, 2, and 4W) after surgery. *Left line*, scrambled decoy ODN–treated side; *right line*, NF-κB decoy ODN–treated side. Defect areas are indicated with white arrows.

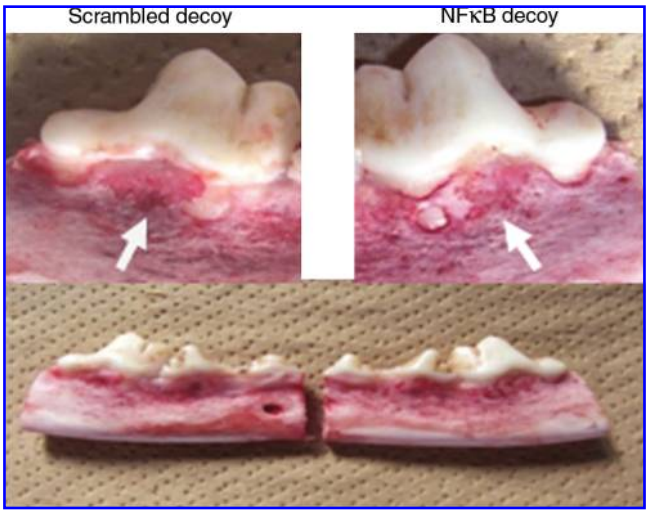

FIG. 7. Macroscopic view of alveolar bone in the bone-defect region at 1 month after surgery, with gingival and periosteal membranes removed. A difference in cortical bone formation is seen in the bifurcation area of the first molars (*white arrows*). *Left panel* shows scrambled decoy ODN–treated side; *right panel* shows NF-κB decoy–treated side. *Upper panel* shows high-magnification view; *lower panel* shows whole-block section.

medium and vitamin D_3 revealed the increased number of TRAP-positive multinucleated cells, whereas NF-κB decoy ODN attenuated them (Fig. 12). These results suggest that NF-κB decoy ODN attenuated osteoclast activity, which secondarily led to osteogenesis.

Discussion

Periodontitis is common disease in the oral region and causes inflammation in alveolar bone. This inflammation induces disattachment of the periodontal ligament, with loosening of the connection between the gingiva and alveolar bone, allowing the extension of bacterial infection such that with *Fusobacterium nuleartum, Actinobacillus actinomycetemcomitans,* and *Porphyromonas gingivalis* (5, 8, 14). To find a new therapeutic strategy for periodontal disease, we used a "decoy" approach in this study, as synthetic dsDNA with a high affinity for transcription factors can be introduced as "decoy" cis-elements to bind transcription factors and block the activation of genes mediating diseases.

A previous study demonstrated that inhibition of NF-κB has therapeutic aspects in both the inhibition of differentiation of osteoclasts in a quantitative manner and the blockade of activation of osteoclasts in a functional manner (20). As for toxicity, NF-κB decoy ODN was preferentially incorporated into monocytes/macrophages in bone marrow co-culture systems, leaving other cells, such as stromal and osteoblast cells, intact; thus, the effect of the decoy was almost limited to osteoclasts and their precursor cells. In this study, NF-κB decoy ODN had no direct effect on osteogenesis in human osteoblast cells but induced osteogenesis by modulating the balance of osteoblast and osteoclast activity in rabbit bone marrow–derived mononuclear cells. Thus, we achieved protection against bone resorption by inhibiting osteoclast differentiation and activation with a minimal amount of NF-κB decoy ODN administration.

In a periodontitis model of debris accumulation, NF-κB decoy ODN administration significantly reduced the concentration of IL-6 in crevicular subgingival fluid. As IL-6, as well as TNF-α, is a well-known inflammatory cytokine that induces osteoclast differentiation, and it is reported to be produced by activated T lymphocytes and macrophages in synovial fluid in rheumatoid arthritis. The accumulation of debris, which allows bacterial infection, is thought to induce an immune response in the local area with migration and activation of responsible cells such as antigen-stimulated lymphocytes and macrophages (4, 6, 8, 24). *P. gingivalis*, a gram-negative bacterium, also expressed potent stimulation of LPS, a component of bacterial cell walls that causes innate immune responses and inflammation. Toll-like receptor 4 (TLR4), a receptor for LPS, activates the MAP/ERK kinase (MEK)/ERK pathway to induce and upregulate RANKL expression in osteoblasts/stromal cells, resulting in enhanced osteoclast formation and function (1, 9, 31). In our results, in human osteoblasts, LPS stimulation induced the expression of pro-inflammatory genes, such as MCP-1, IL-6, and RANKL, which further induced osteoclast formation and activation, and NF-κB decoy ODN treatment attenuated LPS-induced expressions. The mechanisms of NF-κB decoy ODN involved were considered to be a reduction of the immune response on the early inflammatory phase induced by bacterial infection, reduced migration of osteoclast precursor cells in the

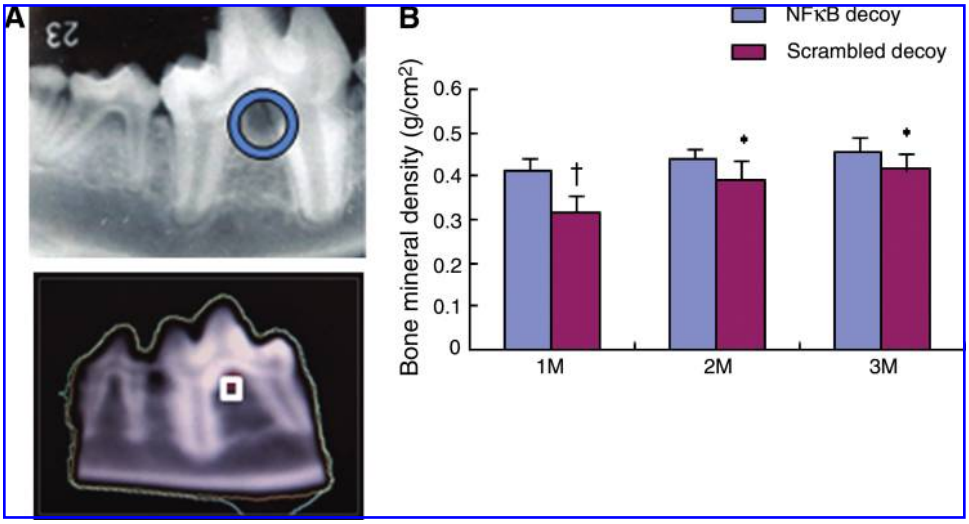

FIG. 8. DEXA analysis of bone mineral density in bone-defect area. (**A**) The area of bone defect under the bifurcation examined is marked with a *circle* on the dental radiographic film (*upper panel*) and with a *square* on the DEXA image (*lower panel*). (**B**) Bone-mineral density (grams per square centimeter) at 1, 2, and 3 months after surgery (1, 2, and 3M). $*p < 0.05$ *versus* NF-κB decoy ODN. $\dagger p < 0.01$ *versus* NF-κB decoy ODN.

crevicular sulcus in the next stage, and direct inhibition of osteoclast differentiation and activation in the late inflammatory phase. In this model, inflammation was continuously maintained with bacterial infection, and destruction and regression of alveolar bone proceeded in a time-dependent manner. Analysis with dental radiographic examination, direct measurement of root-exposure length, and DEXA demonstrated that NF-κB decoy ODN treatment significantly reduced the alveolar bone resorption induced by continuous inflammation.

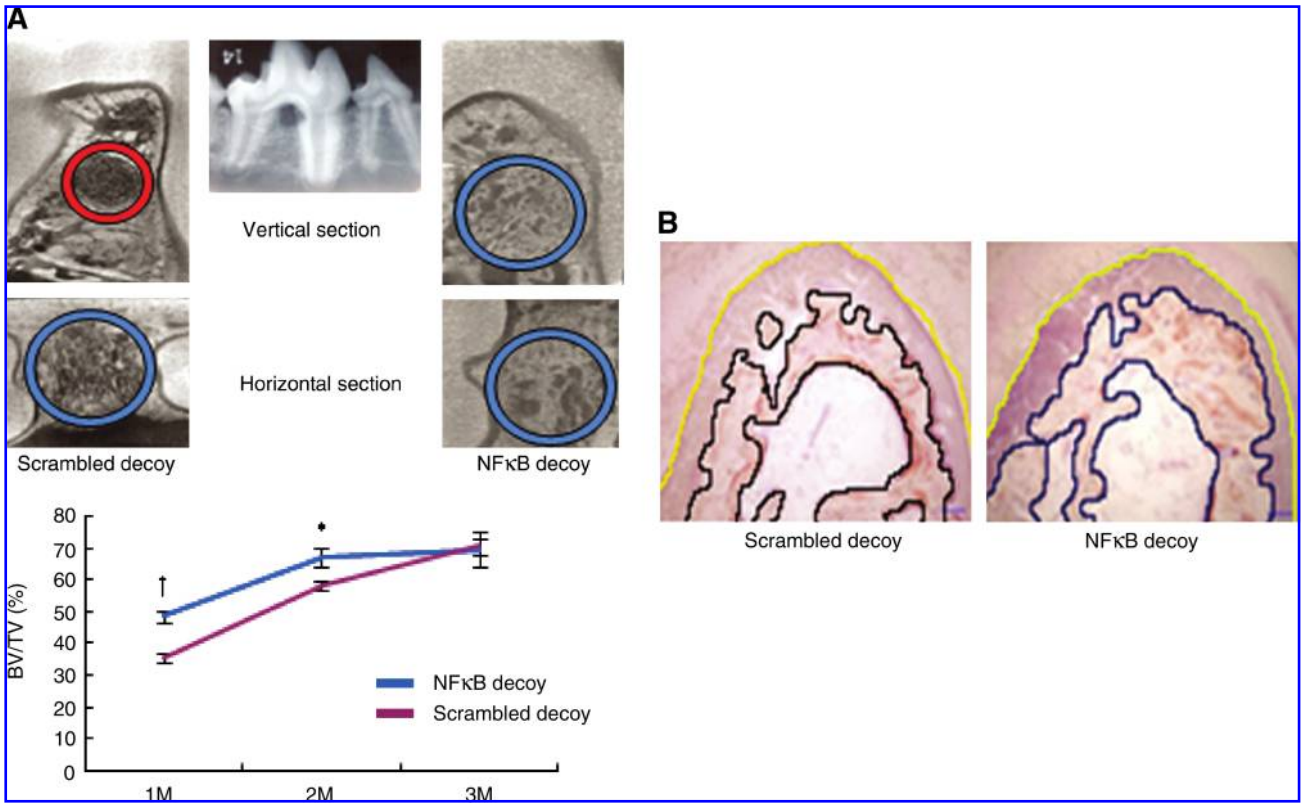

FIG. 9. Micro-CT analysis of bone-defect region. (**A**) *Upper panel:* A reconstruction image of trabecular bone at 1 month after operation. *Left line* shows the scrambled decoy ODN–treated side, and *right line* shows the NF-κB decoy ODN–treated side. A representative dental radiographic film is shown in the center; a lower-magnification image with a *red circle* is shown in the upper left for orientation of the area, and vertical views are shown in the *upper panels* and horizontal views in the lower panels. *Lower panel:* Micro-CT analysis of new trabecular formation as ratio of bone volume to total volume (percentage) in bone-defect region at 1, 2, and 3 months after surgery (1, 2, and 3M). $*p < 0.05$ *versus* scrambled-decoy ODN; $\dagger p < 0.01$ *versus* scrambled decoy ODN. (**B**) Representative photographs of histologic sections of the bone-defect area at 1 month after surgery, with scrambled decoy ODN treatment in the *left panel* and NF-κB decoy ODN treatment in the *right panel*, respectively. (×10 magnification). Calcification area is outlined in black, and root bifurcations in yellow, respectively.

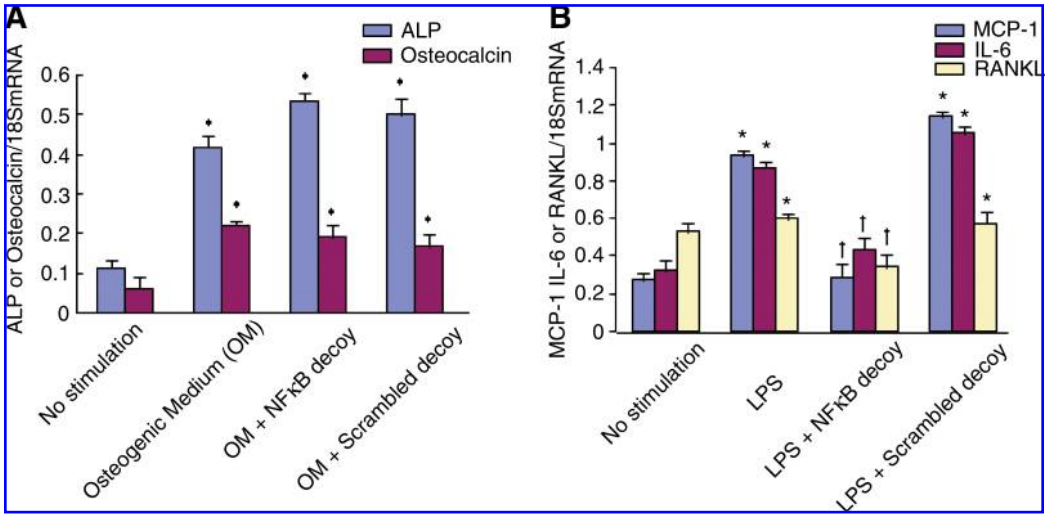

FIG. 10. mRNA quantification by real-time PCR in human osteoblast (A) ALP (*blue bar*) or osteocalcin (*red bar*) mRNA expression after 48-h stimulation with osteogenic medium (OM) in the absence or presence of NF-κB decoy ODN (0.5 μM) or scrambled decoy ODN (0.5 μM). The *bars* represent ALP or osteocalcin mRNA levels relative to 18S mRNA levels. *$p < 0.05$ *versus* no stimulation. (B)MCP-1 (*blue bar*), interleukin-6 (*red bar*), or RANKL (*white bar*) mRNA expression after 24-h stimulation with osteogenic medium (OM) in the absence or presence of NF-κB decoy ODN (0.5 μM) or scrambled decoy ODN (0.5 μM). Each bar shows the target gene level relative to the 18S level. *$p < 0.05$ *versus* no stimulation. †$p < 0.01$ *versus* LPS stimulation.

In the bone-defect model, inflammation is limited in early phase of wound healing of surgical injury without infection; the created bone defect is resorbed initially and will be restored with newly formed trabecular bone with recovery of the three-dimensional architectures. Three-dimensional micro-CT is an ideal approach to examine a selected area with reconstruction of the microtexture of trabecluar formation in the image. Analysis with micro-CT clearly showed a difference at 1 month. This result was supported by dental radiographic examination, which demonstrated obvious calcification in bone-defect area on the NF-κB decoy ODN–treated side (Fig. 8). Histologic evaluation in the mesial–distal plane of block sections also demonstrated that trabecular reconstruction on the NF-κB decoy ODN–treated side was significantly more advanced than that on the scrambled-decoy ODN–treated side at 1 month after operation. As the bone-defect areas analyzed originally consisted of a sponge structure of cancerous bone, micro-CT analysis, which demonstrated a BV/TV of ~70%, suggested that repair in

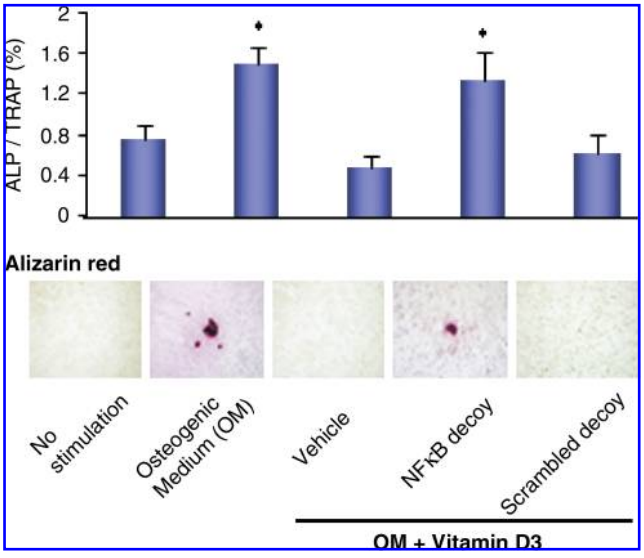

FIG. 11. Effect of NF-κB decoy ODN on *in vitro* calcification model in rabbit bone marrow–derived mononuclear cells. *Upper panel*, ALP-to-TRAP ratio in rabbit bone marrow culture medium at 2 weeks; *lower panel*, the representative pictures of alizarin red staining at 4 weeks (magnification, ×100) with stimulation of osteogenic medium (OM) and/or vitamin D_3 in the absence or presence of NF-κB decoy ODN (0.5 μM) or scrambled decoy ODN (0.5 μM).

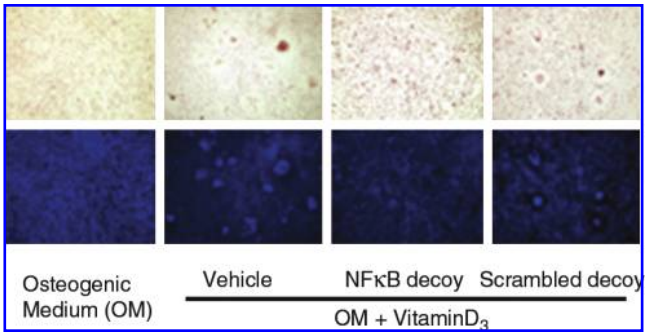

FIG. 12. Effect of NF-κB decoy ODN on the activation of osteoclast in rabbit bone marrow–derived mononuclear cells at 2 weeks. *Upper panel*, the representative pictures of TRAP staining; *lower panel*, Hoechst staining (magnification: ×100) with stimulation of osteogenic medium (OM) and/or vitamin D_3 in the absence or presence of NF-κB decoy ODN (0.5 μM) or scrambled decoy ODN (0.5 μM).

trabecular bone reached a plateau, and the healing process was completed. Together, these results indicate that NF-κB decoy ODNs promote wound healing, inhibiting bone resorption in the early stage, and bringing about wound healing in the next stage of bone formation.

Overall, a decoy approach to block the NF-κB pathway might be a novel approach to prevent bone loss from inflammation with infection as a preventive strategy and to promote wound healing of bone defects as a therapeutic strategy. As the effect of NF-κB on bacterial growth is uncertain at this point, surgical manipulation in combination with antibiotics might be a potential approach to prevent and treat bone metabolic diseases.

Acknowledgments

This work was partially supported by the National Institute of Biomedical Innovation, by a grant-in-aid from the Ministry of Public Health and Welfare, by a grant-in-aid from Japan Promotion of Science, and through Special Coordinated Funds of the Ministry of Education, Culture, Sports, Science and Technology, the Japanese Government.

We thank Ms. Natsuki Yasumasa for technical support and invaluable assistance.

Author Disclosure Statement

No competing financial interests exist.

References

1. Akira S and Takeda K. Toll-like receptor signaling. *Nat Rev Immunol* 4: 499–511, 2004.
2. Cochran DI. Inflammation and bone loss in periodontal diseases. *J Periodontol* 79: 1569–1576, 2008.
3. Farman M and Joshi RI. Full-mouth treatment versus quadrant root surface debridement in the treatment of chronic periodontitis: a systematic review. *Br Dent J* 205:E18; discussion 496–497, 2008.
4. Fujihashi K, Yamamoto M, Hiroi T, Bamberg TV, McGhee JR, and Kiyono H. Selected Th1 and Th2 cytokine mRNA expression by CD4(+)T cells isolated from inflamed human gingival tissues. *Clin Exp Immunol* 10: 422–428, 1996.
5. Garlet GP, Cardoso CR, Silva TA, Ferreira BR, Avila-Campos MJ, Cunha FQ, and Silva JS. Cytokine pattern determines the progression of experimental periodontal disease induced by *Actinobacillus actinomycetemcomitans* through the modulation of MMPs, RANKL and their physiological inhibitors. *Oral/Microbiol Immunol* 21: 12–20, 2006.
6. Han X, Kawai T, Eastcott JW, and Taubman MA. Bacteria-responsive B lymphocytes induce periodontal bone resorption. *J Immunol* 176: 625–631, 2006.
7. Holmstrup P, Poulsen AH, Andersen L, Skuldbøl T, and Fiehn NE. Oral infections and systemic diseases. *Dent Clin North Am* 47: 575–598, 2003.
8. Kawai T, Matsuyama T, Hosokawa Y, Makihira S, Seki M, Karimbux NY, Goncalves RB, Valverde P, Dibart S, Li YP, Miranda LA, Ernst CWO, Izumi Y, and Taubman MA. B and T lymphocytes are the primary source of RANKL in the bone resorptive lesion of periodontal disease. *Am J Pathol* 169: 987–998, 2006.
9. Kikuchi T, Matsuguchi T, Tsuboi N, Mitani A, Tanaka S, Matsuoka M, Yamamoto G, Hishikawa T, Noguchi T, and Yoshikai Y. Gene expression of osteoclast differentiation factor is induced by lipopolysaccharide in mouse osteoblasts via Toll-like receptors. *J Immunol* 166: 3574–3579, 2001.
10. Lohinai Z, Benedek P, Fehér E, Györfi A, Rosivall L, Fazekas A, Salzman AL, and Szabó C. Protective effects of mercaptoethylguanidine, a selective inhibitor of inducible nitric oxide synthase in ligature-induced periodontitis in the rat. *Br J Pharmacol* 83: 353–360, 2004.
11. Martuscelli G, Fiorellini JP, Crohin CC, and Howell TH. The effect of interleukin 11 on the ligature-induced periodontal disease in the beagle dog. *J Periodontol* 71: 573–578, 2000.
12. Mogi M, Otogoto J, Ota N, and Togari A.Differential expression of RANKL and osteoprotegerin in gingival crevicular fluid of patients with periodontitis. *J Dent Res* 83: 166–169, 2004.
13. Murakami S, Takayama S, Ikezawa K, Shimabukuro Y, Kitamura M, Nozaki T, Terashima A, Asano T, and Okada H. Regeneration of periodontal tissues by basic fibrablast growth factors. *J Periodont Res* 34: 425–430, 1999.
14. Nair SP, Meghji S, Wilson M, Reddi K, White P, and Henderson B. Bacterially induced bone destruction: mechanisms and misconceptions. *Infect Immun* 64: 2371–2380, 1996.
15. Ogawa T and Uchida H. A peptide, ALTTE, within the fimbrial subunit protein from *Porphyromonas gingivalis*, induces production of interleukin 6 gene expression and protein phosphorylation in human peripheral blood mononuclear cells. *FEMS Immunol Med Microbiol* 11: 197–206, 1995.
16. Page RC and Kornman KS. The pathogenesis of human periodontitis: an introduction. *Periodontol 2000* 14: 9–11, 1997.
17. Rodrigues DC, Taba MJ, Novaes AB, Souza SL, and Grisi MF. Effect of non-surgical periodontal therapy on glycemic control in patients with type 2 diabetes mellitus. *J Periodontol* 74: 1361–1367, 2003.
18. Sacco G, Carmagnola D, Abati S, Luglio PF, Ottolenghi L, Villa A, Maida C, and Campus G. Periodontal disease and preterm birth relationship. *Minerva Stomatol* 57: 233–246, 2008.
19. Sakallioğlu U, Açikgöz G, Ayas B, Kirtiloğlu T, and Sakallioğlu E. Healing of periodontal defects treated with enamel matrix proteins and root surface conditioning: an experimental study in dogs. *Biomaterials* 25: 1831–1840, 2004.
20. Shimizu H, Nakagami H, Tsukamoto I, Morita S, Kunugiza Y, Tomita T, Yoshikawa H, Kaneda Y, Ogihara T, and Morishita R. NFkappaB decoy oligodeoxynucleotides ameliorates osteoporosis through inhibition of activation and differentiation of osteoclasts. *Gene Ther* 13: 933–941, 2006.
21. Shimizu H, Nakagami H, Osako MK, Hanayama R, Kunugiza Y, Kizawa T, Tomita T, Yoshikawa H, Ogihara T, and Morishita R. Angiotensin II accelerates osteoporosis by activating osteoclasts. *FASEB J* 22: 2465–2475, 2008.
22. Socransky SS, Haffajee AD, Goodson JM, and Lindhe J. New concepts of destructive periodontal disease. *J Clin Periodontol* 11: 21–32, 1984.
23. Sone T, Tamada T, Jo Y, Miyoshi H, and Fukunaga M. Analysis of three-dimensional microarchitecture and degree of mineralization in bone metastases from prostate cancer using synchrotron microcomputed tomography. *Bone* 35: 432–438, 2004.
24. Takayanagi H, Ogasawara K, Hida S, Chiba T, Murata S, Sato K, Takaoka A, Yokochi T, Oda H, Tanaka K, Nakamura K, and Taniguchi T. T cell-mediated regulation of osteoclastogenesis by signaling cross-talk between RANKL and IFN-γ. *Nature* 408: 600–605, 2000.

25. Teng YT, Nguyen H, Gao X, Kong YY, Gorczynski RM, Singh B, Ellen RP, and Penninger JM. Functional human T-cell immunity and osteoprotegerin ligand control alveolar bone destruction in periodontal infection. *J Clin Invest* 106: R59–R67, 2000.
26. Tomita T, Takano H, Tomita N, Morishita R, Kaneko M, Shi K, Takahi K, Nakase T, Kaneda Y, Yoshikawa H, and Ochi T. Transcription factor decoy for NFkappaB inhibits cytokine and adhesion molecule expressions in synovial cells derived from rheumatoid arthritis. *Rheumatology (Oxford)* 39: 749–757, 2000.
27. Tonetti MS, D'Aiuto F, Nibali L, Donald A, Storry C, Parkar M, Suvan J, Hingorani AD, Vallance P, and Deanfield J. Treatment of periodontitis and endothelial function. *N Engl J Med*. 356: 911–920, 2007.
28. Venken K, Boonen S, Van Herck E, Vandenput L, Kumar N, Sitruk-Ware R, Sundaram K, Bouillon R, and Vanderschueren D. Bone and muscle protective potential of the prostate-sparing synthetic androgen 7α-methyl-19-nortestosterone: evidence from the aged orchidectomized male rat model. *Bone* 36: 663–670, 2005.
29. Wara AN, Surarit R, Chayasadom A, Boch JA, and Pitiphat W. RANKL upregulation associated with periodontitis and *Porphyromonas gingivalis*. *J Periodontol* 78: 1062–1069, 2007.
30. Yasuda H, Shima N, Nakagawa N, Yamaguchi K, Kinosaki M, Mochizuki S, Tomoyasu A, Yano K, Goto M, Murakami A, Tsuda E, Morinaga T, Higashio K, Udagawa N, Takahashi N, and Suda T. Osteoclast differentiation factor is a ligand for osteoprotegerin/osteoclastogenesis-inhibitory factor and is identical to TRANCE/RANKL. *Proc Natl Acad Sci U S A* 95: 3597–3602, 1998.
31. Zhang D, Chen L, Li S, Gu Z, and Yan J. Lipopolysaccharide (LPS) of *Porphyromonas gingivalis* induces IL-1 beta, TNF-alpha and IL-6 production by THP-1 cells in a way different from that of *Escherichia coli* LPS. *Innate Immun* 14: 99–107, 2008.

Address correspondence to:
Ryuichi Morishita, M.D., Ph.D.
Professor, Division of Clinical Gene Therapy
Osaka University Graduate School of Medicine
2-2 Yamadaoka, Suita
Osaka 565-0871, Japan

E-mail: morishit@cgt.med.osaka-u.ac.jp

Date of first submission to ARS Central, November 6, 2008; date of final revised submission, January 19, 2009; date of acceptance, January 24, 2009.

Abbreviations Used

ALP = alkaline phosphatase
BMD = bone-mineral density
BV = bone volume
DEXA = dual-photon x-ray absorptiometry
ERK = extracellular signal-regulated kinase
ICAM = intercellular adhesion molecule
MAP = mitogen-activated protein
MCP-1 = monocyte chemotactic protein
M-CSF = macrophage–colony-stimulating factor
MEK = MAPK/ERK kinase
ODF = osteoclast differentiation factor
ODNs = oligodeoxynucleotides
OPG = osteoprotegerin
OPGL = osteoprotegerin ligand
RANK = receptor activator of nuclear factor-kappa B
RANKL = receptor activator of nuclear factor-kappa B ligand
TLR = toll-like receptor
TRANCE = TNF-related activation-induced cytokine
TRAP = tartrate-resistant acid phosphatase
TV = total volume
VCAM = vascular cell adhesion molecule

This article has been cited by:

1. Izumi Aoyama, Ken Yaegaki, Bogdan Calenic, Hisataka Ii, Nikolay Ishkitiev, Toshio Imai. 2012. The role of p53 in an apoptotic process caused by an oral malodorous compound in periodontal tissues: a review. *Journal of Breath Research* **6**:1, 017104. [CrossRef]
2. A R Pradeep, Priyanka N, Nitish Kalra, Savitha B Naik. 2012. "Clinical Efficacy of Subgingivally Delivered 1.2 mg Simvastatin in the Treatment of Subjects with Degree II Furcation Defects: A Randomized Controlled Clinical Trial". *Journal of Periodontology* 1-11. [CrossRef]
3. Roberto Gambari. 2011. Recent patents on therapeutic applications of the transcription factor decoy approach. *Expert Opinion on Therapeutic Patents* **21**:11, 1755-1771. [CrossRef]
4. Jun Jiang, Xiaohong Wu, Minkui Lin, Nghiem Doan, Yin Xiao, Fuhua Yan. 2010. Application of autologous periosteal cells for the regeneration of class III furcation defects in Beagle dogs. *Cytotechnology* **62**:3, 235-243. [CrossRef]
5. Fernando Antunes , Derick Han . 2009. Redox Regulation of NF-#B: From Basic to Clinical Research. *Antioxidants & Redox Signaling* **11**:9, 2055-2056. [Citation] [Full Text HTML] [Full Text PDF] [Full Text PDF with Links]